Journal of the Industrial Technology Research Institute,
Korea Maritime University, Vol. 9, 1991.

Numerical Analysis on Transmittance of Radiative Energy Through Three-Dimensional Packed Spheres

Yong-mo Kim*, Won-yeong Kim, Cheol Oh** and Suck-hun Yoon*****

3차원 粒子層에서의 輻射에너지 透過에 관한 數値解析

金鎔模, 金垣寧, 吳喆, 尹錫勳

抄 錄

몬테카르로수법에 의해 불규칙배열 입자층내의 복사에너지 투과율을 해석하기 위해 불규칙배열 입자층작성 프로그램을 개발하였다. 그 결과는 다음과 같다. (1) 임의의 입자밀도를 갖는 3차원 불규칙배열 입자층작성 프로그램을 개발하였다. (2) 불규칙배열이 가능한 최대 입자밀도는 0.6이다. (3) 이 프로그램은 분자운동해석 및 촉매화확 연소과정 그리고 저진공중에서의 유체흐름을 해석할 수 있다.

1. Introduction

Several devices for the control and utilization of thermal energy have been developed which utilize packed bed or dispersed flow such as high temperature regenerative heat exchanger and droplet radiator for the heat cycles in space stations. The thermal energy is mainly transferred by radiatiom in those systems, whose characteristics were analyzed assuming the packed beds to be continuous [1,2]. Analytical results for radiative transmittance through packed spheres failed to correlate with experimental data[3]. The reason for such a discrepancy was not provided.

The present study is to numerically analyze the radiative transmittance through a vessel filled with randomly packed spheres of equal diameter by a Monte Carlo method. The effects of the side

* Hokkaido University, Sapporo 060, Japan
** Korea Maritime University, Pusan 606, Korea
*** National Fisheries University of Pusan, Pusan 608, Korea

walls on the radiative transmittance are taken into account. A computer program is developed for generating the pattern of three-dimensional, randomly packed spheres.

Two methods are proposed to radomly pack the spheres in a three-dimensional space : one is to directly pack them in a random manner, while the other is to randomly rearrange an initially, regularly packed system. Typical examples of the former method are : (i) to place the spheres at an arbitrary location (x, y, z), which is determined by the multiple sets of three random numbers, with the spheres not intersecting with those in the previous set [4], and (ii) the slowly settling sphere model [5]. The method (i) takes an extremely long computation time to determine a random arrangement in a packed bed with higher packing density. The slowly settling sphere model (ii) can produce only an arrangement called loose random packing with a packing density of approximately 0.5-0.6, which cannot be chosen arbitrarily. The method of random rearranging initially, regularly packed spheres is used to determine the relation between several transfer coefficients and the inter-molecular force [6]. It simulates the kinetics of individual molecules by a Monte Carlo method. A computer program is developed to generate a three-dimensional, random packing of regularly arranged spheres with arbitrary packing density.

2. Procedure to Obtain Randomly Packed Spheres

2. 1 general flow

The analysis is performed on a parallelepiped whose dimension is depicted in Fig. 1. Initially, spheres of equal diameter are placed at the lattice points of each face-centered lattice. Lattices are uniformly stocked in the parallelepiped region whose dimensions are XL by YL by ZL. The diameter of each sphere is

$$D = \{(6C \cdot XL \cdot YL \cdot ZL)/(IT \cdot \pi)\}^{1/3} \tag{1}$$

Here, C is the packing density, and IT is the total number of spheres in the region whose dimension is determined by

$$YL = (\sqrt{3/2})\, XL \tag{2}$$

$$ZL = (\sqrt{2/3})\, XL \tag{3}$$

The parallelepiped is surrounded by similar ones which repeat consecutively outward to infinity. With this system structure, the computer needs to memorize the position of spheres in only one parallelepiped.

Now, the analysis begins with a regualr arrangement of spheres in the parallelepiped. These

spheres are then moved in there-dimensional random directions, one by one following the procedure described in Fig. 2.

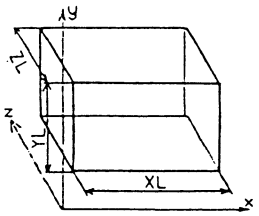

Fig. 1 System Boundary of parallelepiped Region

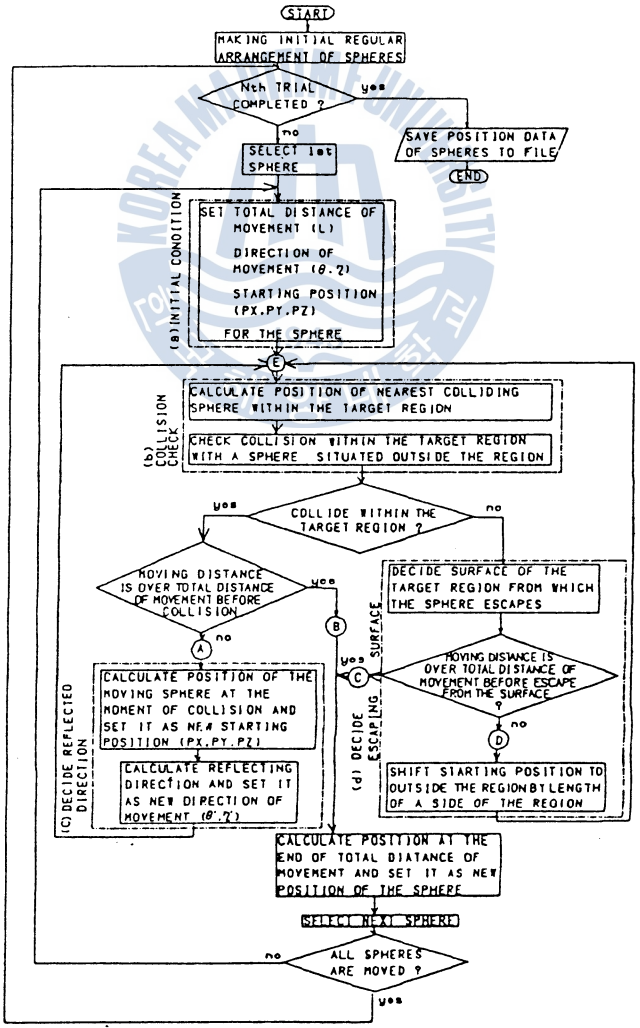

Fig. 2 Flow Chart for Computational procedure

When one sphere collides with another, it is deflected as in an elastic collision, and travels a length L which is randomly determined. When it comes to a stop, the movement of the next sphere is started, After all spheres are tried, the procedure is resumed with the first sphere. With N repetitions, the final positions of the spheres are stored to be used in the subsequent calculation for radiative transmittance.

The programing in Fig. 2 can be grouped into four parts: (a) a routine to determine the moving direction and the travel length of spheres. (b) a routine to search th first struck sphere in the target region, (c) a rotuine to decide the direction of deflection after collision, and (d) a routine to determine the terminal of a sphere in case of no collision and to move it to the destination. Details of the routines are presented in the following:

2. 2 initial conditions of movement

The moving direction of the sphere is determined randomly by using two uniform random numbers between 0 and 1, namely RND1 and 2 [7] as

$$\theta = 2\ \pi \cdot RND1 \tag{4}$$

$$\eta = cos^{-1}(1-2 \cdot RND2) \tag{5}$$

Here, θ and η are the angles defined in Fig. 3. The total travel length is obtained by another random number, RND3 as

$$L = LMAX \cdot RND3 \tag{6}$$

where, LMAX is the maximum total travel length which is given initially.

2. 3 idientifying the first struck sphere

Consider two adjacent regions, "firing" region (i) from which the tracer sphere is originated and "foreign" region(ii). The tracer sphere has four possible collision cases: (i) with a "domestic" sphere in the firing region, (ii) with a "foreign" sphere in the firing region, as shown in Fig. 4, (iii) with a "domestic" sphere in the foreign region, as shown in Fig. 5, and (iv) with a "foreign" sphere in the foreign region. Here, (PX, PY, PZ) and (PXN, PYN PZN) denote the initial and colliding locations of the tracer, respectively, and (PX′, PY′, PZ′) is the colliding location of the collided sphere. Two routines are in the computer program: One is to test the collision case(i) and the other to examine case (ii).

The two routines treat case (iii) as no collision, while case (iv) is treated like case (ii). Figure 6 depicts the way to determine the first struck sphere. The sphere initially at A (PX, PY, PZ) moves

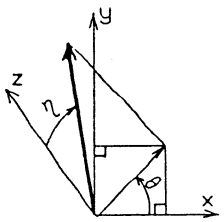

Fig. 3 Moving Direction of Sphere

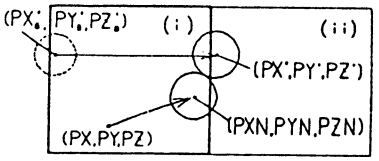

Fig. 4 Collision with in a Firing Region

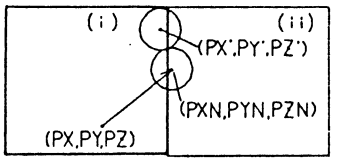

Fig. 5 Collision outside a Firing Region

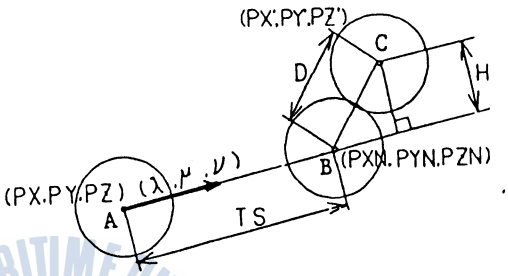

Fig. 6 Collision Length

to a new position B (PXN, PYN, PZN), with the directional cosines of (λ, μ, ν), as detetmined by Eqs. (4) and (5). Here,

$$\lambda = cos\theta sin\eta \tag{7}$$

$$\mu = sin\theta sin\eta \tag{8}$$

$$\sigma = cos\eta \tag{9}$$

Let H be the distance from the center of a sphere C to the line AB and TS be the distance between A and B. Here,

$$H = \{(PX'-PX)^2+(PY'-PY)^2+(PZ'-PZ)^2-TSL^2\}^{1/2} \tag{10}$$

$$TS = TSL \quad -\sqrt{D^2-H^2} \tag{11}$$

$$TSL = \lambda(PX'-PX)+\mu(PY'-PY)+\nu(PZ'-PZ) \tag{12}$$

If H is smaller than the diameter D and TS is positive and takes the minimum value, the sphere is the first one to collide with the tracer sphere.

Next, the center of a collided sphere (PX′, PY′, PZ′) situated in the "foreign" region is determined in order to ascertain a collision with the tracer sphere in the "firing" region, as shown in Fig. 4. Such a collided sphere gas its center in the peripheral region surrounding the "firing" region (i) with the width of D. as illustrated in Fig. 7. When the travel distance of the tracer sphere is less than L defined by Eq. (6) at collision, it collides with the sphere and rebounds at the surface (branch flow A in Fig. 2). When the travel distance exceeds L, the tracer sphere stops after travelling a distance L (branch flow B in Fig. 2) and proceeds to move to the next sphere.

2. 4 reflection

When the tracer sphere collides with a sphere (PX′, PY′, PZ′) at the point (PXN, PYN, PZN), it is reflected in the new direction (λ', μ', ν'), as shown in Fig. 8. Here,

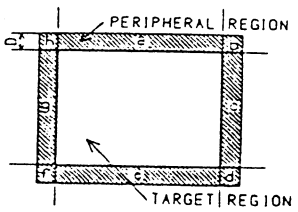

Fig. 7 Peripheral Region

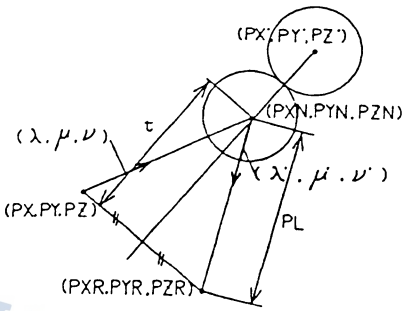

Fig. 8 Reflected Direction

$$\lambda' = (PXR - PXN)/PL \tag{13}$$

$$\mu' = (PYR - PYN)/PL \tag{14}$$

$$\nu' = (PZR - PZN)/PL \tag{15}$$

$$PL = \{(PXR - PXN)^2 + (PYR - PYN)^2 + (PZR + PZN)^2\}^{1/2} \tag{16}$$

$$PXR = 2(PXN + ut) - PX \tag{17}$$

$$PYR = 2(PYN + yt) - PY \tag{18}$$

$$RZR = 2(PZN + wt) - PZ \tag{19}$$

$$t = \{u(PX - PXN) + v(PY - PYN) + w(PZ - PZN)\}/(u^2 + v^2 + w^2) \tag{20}$$

$$u = PX' - PXN \tag{21}$$

$$v = PY' - PYN \tag{22}$$

$$w = PZ' - PZN \tag{23}$$

After reflection, the computational flow path in Fig. 2 returns to point E, and a search for the first struck sphere begins.

2. 5 moving to outside "firing" region

When the tracer sphere misses collision within the "firing" region, it travels into the "foreign" region, and a search for the first struck sphere in the new region is continued. When the travel distance of the tracer sphere reaches L, determined by Eq. (6), the sphere comes to a stop at the point (branch flow C in Fig. 2).

2. 6 numerical examples of randomly packed spheres

Figure 9 shows a cube filled with regularly packed spheres with a packing density of 0.55. Figures 10 depicts the sectional view of the packed spheres along the X-Y plane. An example of randomly packed spheres with a packing density of 0.55 is depicted in Fig. 11. Figures 12 also illustrates the sectional view of the rendomly packed spheres. The average radial distribution function G(R) is incorporated to indicate the randomness of the spheres [4,6]. Its definition is

(average number of spheres which have their centers between R to R+dR from the center of each sphere)

$$=4\pi R^2 dR \cdot N \cdot G(R) \tag{24}$$

where, N is the average number density of spheres. Hence, the function G(R) represents the average ratio of the real number density to the average density at a distance R from the center of each sphere.

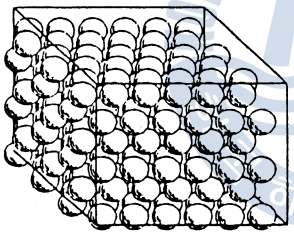

Fig. 9 Numerical Result of Regular Arrangement (C=0.55)

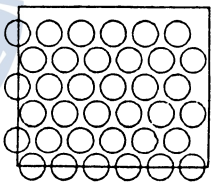

Fig. 10 Cross-sectional View of Regular Arrangement (C=0.55)

When the value of the function is unity and independent from R, the arrangement of the spheres is completely random.

Figure 13 shows the average radial distribution function G(R) of the packed spheres with regular arrangment shown in Fig. 9. This curve has many peaks even at a remote distance from each sphere indicating an arrangement with strong regularity. Figure 14 shows the function of packed spheres in random arrangement as shown in Fig. 11. The value of G(R) is practically unity except in the vicinity of a sphere. This implies that the arrangement lacks a long range regularity. The deviation from unity at the left end of the curve indicates the existence of some regularity near the surface of each sphere. The observation can be explained by the fact that no sphere can intersect with other spheres. This phenomenon can be observed in the results of the slowly settling sphere model [5] and in the experiment of steel spheres packed in a rubber bag [8].

Figure 15 shows the sectional view of randomly packed spheres with a packing density of 0.6. The packing density differs from section to section, but maintains a regularity at the sections with higher packing density as shown in Fig. 15.

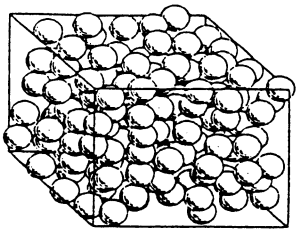

Fig. 11 Numerical Result of Random Arrangement (C=0.55)

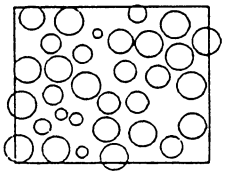

Fig. 12 Cross-sectional View of Random Arrangement (C=0.55)

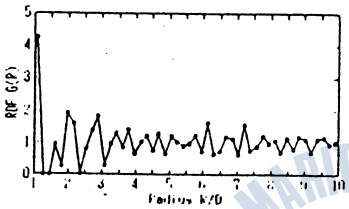

Fig. 13 Average Radial Distribution Function for Random Arrangement (C=0.55)

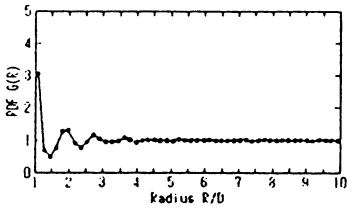

Fig. 14 Average Radial Distribution Function for Random Arrangement (C=0.55)

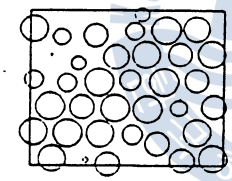

Fig. 15 Cross-sectional View of Semi-random Arrangement (C=0.6)

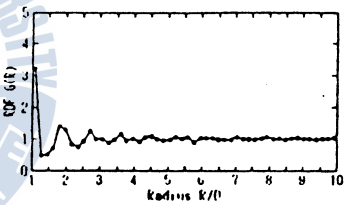

Fig. 16 Average Radial Distri-bution Function for Semi-random Arrangement (C=0.6)

Figure 16 depicts the average radial distribution function of this arrangement, which shows some regularity at a larger distance from the surface of each sphere. This corresponds to the case where latex spheres with a diameter of around 0.05-1 micron begin to form a regular arrangement in water with a packing density over 0.5-0.55[6].

3. Analyses on Transmittance Through Packed Spheres

In analyzing the transmittance of radiative energy through the packed spheres whose arrangement is determined by the previous section, radiative energy is diffusely emitted from a surface which is parallel to the $z=0$ wall of the parallelepiped region at a distance of 0.5D, as shown in Fig. 17. The emission of radiative energy is simulated by a large number of energy bundles emitted from many arbitrarily chosen points (x_0, y_0) on the surface in the direction dictated by Lambert's cosine law. The position (x_0, y_0), the angle between the Z axis and each

direction of energy bundle, and the angle η between the X axis and the projected direction of energy bundle on the X-Y plane are obtained through the use of four random numbers (RND1-4) as

$$(x_0,\ y_0) = (RND1 \cdot XL,\ RND2 \cdot Y_L) \tag{25}$$

$$\gamma = (1/2)\cos^{-1}(1-2 \cdot RND3) \tag{26}$$

$$\eta = 2\pi \cdot RND4 \tag{27}$$

After the emission of energy bundle, its collision with spheres or the side walls of the region is checked. When it strikes the side walls, two boundary conditions are considered : one is a periodic boundary and the other is a specular one. In the periodic boundary case, the striking energy bundle is reemitted from the opposite side wall in the direction parallel to the one before collision. In the case of speclar boundary, the striking energy bundle is reflected by the wall.

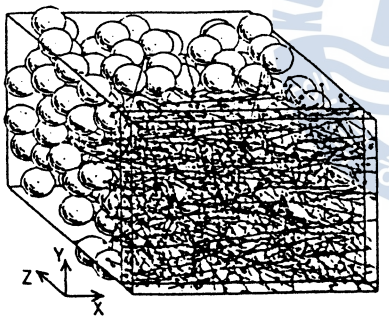

Fig. 17 Simulation of Radiative Transmittance in Packed Spheres

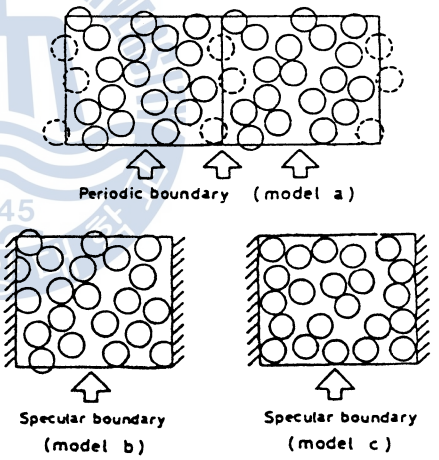

Fig. 18 Models of Randomly Packed Spheres

For the periodic boundary, the spheres have the same arrangements in every region, as shown in Fig. 18 (model a), which simulates the packed spheres of infinite width. For the specular boundary, however, two models, (model b and c), are considered, as shown in Fig. 18. In the (model b), the intruded part of each sphere is cut off, while in the (model c), all spheres are arranged to situate inside the region. The local packing densities of the (models b and c) at the narrow zone along the side walls are lower than that of the (model a), as shown in Fig. 19. The (models b and c) simulate the actual experimental system [3] with specular side walls and low packing density zone along the side walls. In the (model c), certain variation in the packing density is observed in Fig. 19, due to the aligning effect of spheres [8]. The energy bundles incident on the spheres are either reflected or absorbed, whose probability depends on the emissivity of the surface. Specular reflection is considered in the analysis.

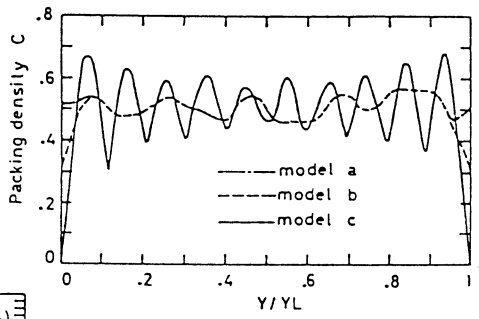

Fig. 19 Profiles of Local Packing Density

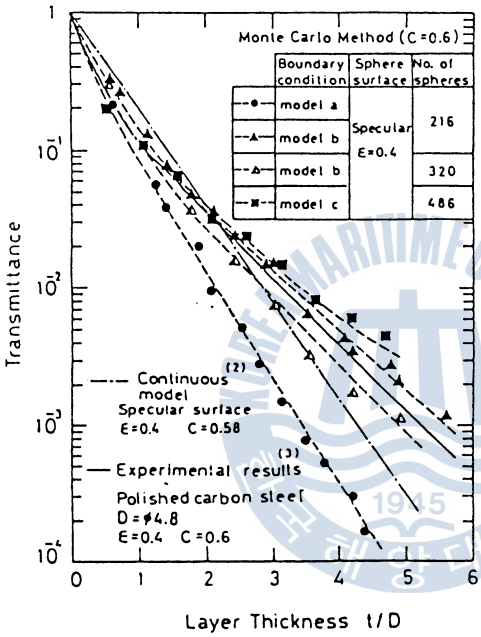

Fig. 20 Radiative Transmittance through Packed Spheres

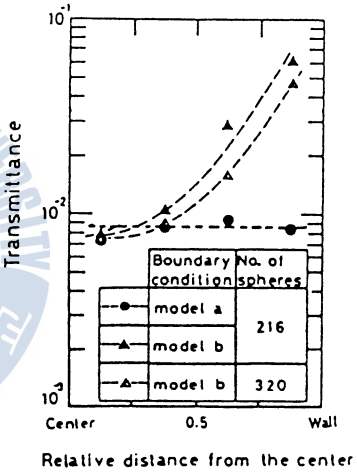

Fig. 21 Profiles of Radiative Transmittance

4. Numerical Results and Discussion

Figure 20 depicts the numerical results of radiative transmittance through the packed spheres with specular surfaces and the packing density of 0.6. The experimental result of Churchill et al. [3] and the numerical one of Howell et al. by the continuous model [2] are also depicted in Fig. 20. The variable t/D for the horizontal axis represents the non-dimensional thickness of the bed. The slope of the experimental results on transmittance decreases at t/D=1-2, which is not appeared in Howell's results.

In the present study with low packing density zone along the side walls, the reduction in transmittance in the (models b and c) is much less than that in the (model a) with infinite width. Figure 20 also depicts that the (models b and c) yield the inflection of the transmittance curve at

t/D=1−2. For the sake of investigating the wall effect, the profiles of the transmittance are plotted in Fig. 21 at a section of t/D=2.2−2.3. These profiles depict that transmittance in the (model a) is uniform due to the infinite width, and that the transmittance in the (model b) is higher in the vicinity of side walls due to the existence of the near-wall low packing density zone. This effect appears higher in the packed bed which contains the smaller number of spheres. Hence, the characteristics of radiative transmittance in the (models b and c) can be explained by the combined effect of the highly attenuating central region and of the peripheral region with lower attenuation. To show the difference in the transmittance between these two regions, the numerical results of the (model b) with 320 spheres is depicted in Fig. 20. Compared with the results for 216 spheres, the increase in transmittance of 320 spheres is somewhat reduced resulting from an increase in the cross-sectional area of radiative energy transmittance. It implies that, in measuring the transmittance of packed spheres, the distance between the side walls should be wide enough relative to the sphere diameter in order to reduce the side-wall effects.

The numerical result obtained from the (model c) is superimposed in Fig. 20. It agrees well with the experimental results of Churchill et al..

5. Conclusions

(1) A computer program is developed for the arrangement of equal-diameter spheres in a packed bed with arbitrary packing density. It is shown that this program can make random arrangement for the beds with a packing density less than 0.6.

(2) The low packing density zone adjacent to the side walls causes a decrease in the bed beginning at the 1-2 diameter depth from the surface of radiation entrance.

(3) An empty space between the side walls and the packed body of an approximately 10-diameter width contributes to an increase in the transmittance of radiative energy by an order of magnitude. The enhancement effect diminishes with an increase in the cross-sectional area of the packed bed perpendicular to the direction of radiative transmittance.

The authors wish to acknowledge the financial support from the Science Foundation in Japanese Ministry of Education under number C (62550140). A part of the numerical computations was performed at the Hokkaido University Computing Center.

References

1) Brewster, M.Q. and Tien, C.L., Radiative Transfer in Packed Fluidized Beds: Dependent versus Independent Scattering, Trans. ASME, J. of Heat Transfer, 104, 11, 573-579(1982).
2) Yang, Y.S., Howell, J.R. and Klein, D.E., Radiative Heat Transfer Through a Randomly Packed Bed of Spheres by the Monte Carlo Method, Trans. ASME, J. Heat Transfer, 105, 5, 325-332(1983).
3) Chen, J.C. and Churchill, S.W., Radiant Heat Transfer in packed Beds, AICHE.J., 9, 1, 35-41(1963).
4) Goto, K., Liquid and Powder Engng., 15, 4, 220-226(1978) (in Japanese).
5) Jodrey, W.S. and Tory, E.M., Simulation of Random Packing of Spheres, Simulation, 1-12(Jan.-1979).
6) Toda, M. et al., The Structure and the Characteristics of Liquids, (1976), Iwanami (in Japanese).
7) Kudo, K. et al., Monte Carlo Method for Radiative Heat Transfer Analysis of General Gas-Particle Enclosures, Proc. 5th Int. Conf, on Numerical Method in Thermal Problems, V, 2, 1264-1275(1987).
8) Bernal; J.D., The Structure of Liquids, Proc. Roy. Soc., A, 280, 299-322(Jul.-1964)